

# Syntheses and characterization of $\text{Cp}_2\text{Ce}[\eta^3\text{-N}(\text{QPPH}_2)_2]$ ( $\text{Q} = \text{S}, \text{Se}$ ) and $\text{Cp}_2\text{Ce}[\eta^3\text{-N}(\text{SP}^i\text{Pr}_2)(\text{SePPh}_2)]$

Perumal Sekar, James A. Ibers \*

*Department of Chemistry, Northwestern University, 2145 Sheridan Road, Evanston, IL 60208-3113, United States*

Received 30 September 2005; accepted 17 October 2005

Available online 5 January 2006

Dedicated with admiration to Prof. Brian James on the occasion of his 70th birthday (JAI).

## Abstract

The compounds  $\text{Cp}_2\text{Ce}[\eta^3\text{-N}(\text{QPPH}_2)_2]$  ( $\text{Q} = \text{S}$  (**1**),  $\text{Se}$  (**2**)) and  $\text{Cp}_2\text{Ce}[\eta^3\text{-N}(\text{SP}^i\text{Pr}_2)(\text{SePPh}_2)]$  (**3**) have been synthesized from the protonolysis reactions between  $\text{Cp}_3\text{Ce}$  and  $\text{HN}(\text{QPPH}_2)_2$  or  $\text{HN}(\text{SP}^i\text{Pr}_2)(\text{SePPh}_2)$  in THF. The structures of these compounds have been determined by X-ray crystallographic methods. The three compounds have similar structures in which the ligands are coordinated to  $\text{Cp}_2\text{Ce}$  moiety in an  $\eta^3$  fashion through the two chalcogen atoms and an N atom. Whereas the  $^{77}\text{Se}$  NMR resonances are normal the  $^{31}\text{P}$  NMR resonances are shifted to much lower frequencies than in similar rare-earth compounds.

© 2005 Elsevier B.V. All rights reserved.

**Keywords:** Rare-earth metal complexes; Imidodiphosphinodichalcogenido ligands; Crystal structures

## 1. Introduction

In recent years, metal complexes of imidodiphosphinodichalcogenido ligands,  $[\text{N}(\text{QPR}_2)_2]^-$ , ( $\text{Q} = \text{S}, \text{Se}$ ;  $\text{R} =$  organic group), have been widely used as molecular single-source precursors for the preparation of thin films, nanoparticles, or quantum dots by chemical vapor deposition or solution methods [1–4]. These single-source precursors obviate the need for highly toxic sources of chalcogenides, such as  $\text{H}_2\text{S}$  or  $\text{H}_2\text{Se}$ , in the synthesis of solid-state compounds or nanomaterials. We have previously reported the coordination chemistry of  $[\text{N}(\text{QPPH}_2)_2]^-$  ( $\text{Q} = \text{S}$  and  $\text{Se}$ ) ligands with rare-earth metal salts ( $\text{Ln} = \text{Y}, \text{Yb}, \text{La}, \text{Gd},$  and  $\text{Er}$ ) [5–7]. We have found that these ligands are coordinated to the metal centers either through the two Q atoms ( $\eta^2$  coordination) or more commonly through the two Q atoms and the N atom ( $\eta^3$  coordination). To understand the bonding motifs further, we have stu-

died the coordination toward  $\text{Cp}_3\text{Ce}$  of the  $[\text{N}(\text{QPPH}_2)_2]^-$  ( $\text{Q} = \text{S}, \text{Se}$ ) and  $\text{HN}(\text{SP}^i\text{Pr}_2)(\text{SePPh}_2)$  ligands. In this paper, we report the syntheses, NMR spectroscopy, and X-ray crystal structures of  $\text{Cp}_2\text{Ce}[\eta^3\text{-N}(\text{SPPH}_2)_2]$  (**1**),  $\text{Cp}_2\text{Ce}[\eta^3\text{-N}(\text{SePPh}_2)_2]$  (**2**), and  $\text{Cp}_2\text{Ce}[\eta^3\text{-N}(\text{SP}^i\text{Pr}_2)(\text{SePPh}_2)]$  (**3**).

## 2. Experimental

### 2.1. General procedures

All manipulations were performed under an inert atmosphere of  $\text{N}_2$  with the use of standard Schlenk-line techniques or under Ar in a glovebox. Solvents were dried, distilled, and degassed under  $\text{N}_2$  before use. Anhydrous  $\text{Et}_2\text{O}$  and THF were distilled from Na and benzophenone; pentane and  $\text{CH}_2\text{Cl}_2$  were distilled from  $\text{P}_2\text{O}_5$ .  $\text{Cp}_3\text{Ce}$  was purchased from Strem Chemical Co. (Newburyport, MA) and used as received. The compounds  $\text{HN}(\text{SPPH}_2)_2$ ,  $\text{HN}(\text{SePPh}_2)_2$ , and  $\text{HN}(\text{SP}^i\text{Pr}_2)(\text{SePPh}_2)$  were prepared according to the literature methods [8–11]. NMR data on  $\text{CH}_2\text{Cl}_2/\text{CD}_2\text{Cl}_2$  solutions of **1–3** were recorded on

\* Corresponding author. Fax: +1 847 491 5449.

E-mail address: [ibers@chem.northwestern.edu](mailto:ibers@chem.northwestern.edu) (J.A. Ibers).

either a Mercury 400 MHz spectrometer ( $^{31}\text{P}$  with a 5 mm NMR probe) or an INOVA 400 MHz spectrometer ( $^{77}\text{Se}$  with a 10 mm broad-band NMR probe).  $^{31}\text{P}$  chemical shifts, in ppm, were recorded at 166.994 MHz and were referenced to an external standard of 85%  $\text{H}_3\text{PO}_4$  (set to 0 ppm).  $^{77}\text{Se}$  chemical shifts, in ppm, were recorded at 76.287 MHz and referenced to an external standard of a saturated solution of  $\text{Ph}_2\text{Se}_2$  in  $\text{CD}_2\text{Cl}_2$  (set to 460 ppm). An electrospray mass spectrum was obtained on a Micromass Quattro II instrument. Elemental analyses were performed by Oneida Research Services, Whitesboro, NY.

## 2.2. Synthesis of $\text{Cp}_2\text{Ce}[\eta^3\text{-N}(\text{SPPPh}_2)_2]$ (**1**)

$\text{Cp}_3\text{Ce}$  (0.168 g, 0.50 mmol) dissolved in THF (10 mL) was added slowly to a solution of  $\text{HN}(\text{SPPPh}_2)_2$  (0.225 g, 0.50 mmol) in THF (10 mL). After the reaction mixture was stirred for 1 h, the volume of the resultant brown solution was reduced to 10 mL under vacuum and 10 mL of pentane was added. The solution produced large clear crystals of  $\text{Cp}_3\text{Ce}(\text{THF})$  upon sitting overnight at  $-10^\circ\text{C}$ . The THF/pentane solution was filtered into a reaction flask and the solvent was removed under vacuum. The residue was dissolved in  $\text{CH}_2\text{Cl}_2$ , layered with  $\text{Et}_2\text{O}$ , and then kept at  $-10^\circ\text{C}$  overnight. Crystals of **1** were isolated along with unreacted  $\text{HN}(\text{SPPPh}_2)_2$ . We were not able to obtain satisfactory elemental analyses owing to the presence of this unreacted  $\text{HN}(\text{SPPPh}_2)_2$ . However, EDX analyses of single crystals of **1** confirmed the presence of Ce, P, and S in approximately 1:2:2 ratios.  $^{31}\text{P}\{^1\text{H}\}$  NMR ( $\text{CH}_2\text{Cl}_2/\text{CD}_2\text{Cl}_2$ ,  $25^\circ\text{C}$ ):  $\delta$   $-40.6$ .  $^1\text{J}_{\text{P-Se}} = 538$  Hz).

## 2.3. Synthesis of $\text{Cp}_2\text{Ce}[\eta^3\text{-N}(\text{SePPh}_2)_2]$ (**2**)

$\text{Cp}_2\text{Ce}[\eta^3\text{-N}(\text{SePPh}_2)_2]$  was synthesized in a manner similar to that described for the synthesis of **1** but with the addition of  $\text{HN}(\text{SePPh}_2)_2$  in place of  $\text{HN}(\text{SPPPh}_2)_2$ . Yellow crystals of **2** were obtained by recrystallization from  $\text{CH}_2\text{Cl}_2$  at  $0^\circ\text{C}$ . Yield: 0.20 g, 49%. *Anal.* Calc. for  $\text{C}_{34}\text{H}_{30}\text{CeNP}_2\text{Se}_2$ : C, 50.26; H, 3.72; N, 1.72. Found: C, 49.76; H, 3.60; N, 1.95%.  $^{31}\text{P}\{^1\text{H}\}$  NMR ( $\text{CH}_2\text{Cl}_2/\text{CD}_2\text{Cl}_2$ ,  $25^\circ\text{C}$ ):  $\delta$   $-64.6$  ( $^1\text{J}_{\text{P-Se}} = 538$  Hz).  $^{77}\text{Se}\{^1\text{H}\}$  NMR ( $\text{CH}_2\text{Cl}_2/\text{CD}_2\text{Cl}_2$ ,  $25^\circ\text{C}$ ):  $\delta$  37.8 (d,  $^1\text{J}_{\text{Se-P}} = 609$  Hz). ESI-MS ( $\text{CH}_2\text{Cl}_2$ )  $\{m/z$  (%) [assignment]  $\}$ : 544 (100)  $[\text{N}(\text{SePPh}_2)_2]^+$ , 464 (4)  $[\text{NSe}(\text{PPh}_2)_2]^+$ , 430 (9)  $[\text{Cp}_2\text{CeSe}_2]^+$ , 386 (24)  $[\text{HN}(\text{PPh}_2)_2 + \text{H}^+]$ , 350 (30)  $[\text{Cp}_2\text{CeSe}]^+$ .

## 2.4. Synthesis of $\text{Cp}_2\text{Ce}[\eta^3\text{-N}(\text{SP}^i\text{Pr}_2)(\text{SePPh}_2)]$ (**3**)

$\text{Cp}_2\text{Ce}[\eta^3\text{-N}(\text{SP}^i\text{Pr}_2)(\text{SePPh}_2)]$  was synthesized in a manner similar to that described above for **1** except for the use of  $\text{HN}(\text{SP}^i\text{Pr}_2)(\text{SePPh}_2)$  in place of  $\text{HN}(\text{SPPPh}_2)_2$ . The synthesis afforded yellow crystals of **3** along with clear crystals of  $\text{HN}(\text{SP}^i\text{Pr}_2)(\text{SePPh}_2)$ . EDX analysis confirmed the presence of Ce, P, S, and Se in approximately a 1:2:1:1 ratio.

We were not able to obtain elemental analyses because of insufficient crystalline material and the presence of unreacted  $\text{HN}(\text{SP}^i\text{Pr}_2)(\text{SePPh}_2)$ .  $^{31}\text{P}\{^1\text{H}\}$  NMR ( $\text{CH}_2\text{Cl}_2/\text{CD}_2\text{Cl}_2$ ,  $25^\circ\text{C}$ ):  $\delta$   $-52.5$ , 18.7.  $^{77}\text{Se}\{^1\text{H}\}$  NMR ( $\text{CH}_2\text{Cl}_2/\text{CD}_2\text{Cl}_2$ ,  $25^\circ\text{C}$ ):  $\delta$  86.6 (d,  $^1\text{J}_{\text{Se-P}} = 590$  Hz).

## 2.5. Crystallographic studies

Single-crystal X-ray diffraction data were collected at 153 K on a Bruker 1000 CCD X-ray diffractometer with the program SMART [12] at 153 K with the use of monochromatized Mo  $\text{K}\alpha$  radiation ( $\lambda = 0.71073$  Å). The diffracted intensities generated by a scan of  $0.3^\circ$  in  $\omega$  were recorded on four sets of 606 frames at  $\phi$  settings of  $0^\circ$ ,  $90^\circ$ ,  $180^\circ$ , and  $270^\circ$ , with an additional 50 frames at  $\phi = 0^\circ$  for detection of possible decay. The exposure times were 10 s/frame for **1** and **2**, and 20 s/frame for **3**. Cell refinement and data reduction were carried out with the use of the program SAINT [12]. Face-indexed absorption corrections were made with the program XPREP [13]. Then, the program SADABS was employed to make incident beam and decay corrections [12]. The structures were solved by direct methods with the program SHELXS and refined by full-matrix least-squares techniques with the program SHELXL [13]. Hydrogen atoms were generated in calculated positions and constrained with the use of a riding model. The final models involved anisotropic displacement parameters for all non-hydrogen atoms. Selected crystallographic data for **1–3** are listed in Table 1 and further crystallographic details may be found in Supplementary data. Selected bond distances and angles for **1–3** are listed in Table 2.

Table 1  
Selected crystallographic data for  $\text{Cp}_2\text{Ce}[\eta^3\text{-N}(\text{SPPPh}_2)_2]$  (**1**),  $\text{Cp}_2\text{Ce}[\eta^3\text{-N}(\text{SePPh}_2)_2]$  (**2**), and  $\text{Cp}_2\text{Ce}[\eta^3\text{-N}(\text{SP}^i\text{Pr}_2)(\text{SePPh}_2)]$  (**3**)

	<b>1</b>	<b>2</b>	<b>3</b>
Formula	$\text{C}_{34}\text{H}_{30}\text{CeNP}_2\text{S}_2$	$\text{C}_{34}\text{H}_{30}\text{CeNP}_2\text{Se}_2$	$\text{C}_{28}\text{H}_{34}\text{CeNP}_2\text{SSe}$
Formula mass	718.77	812.57	697.64
Space group	$P\bar{1}$	$P\bar{1}$	$P2_1/c$
$a$ (Å)	9.817(2)	9.797(2)	9.618(2)
$b$ (Å)	12.323(3)	12.396(3)	33.658(7)
$c$ (Å)	13.840(3)	13.933(3)	9.375(2)
$\alpha$ ( $^\circ$ )	88.12(3)	88.11(3)	90
$\beta$ ( $^\circ$ )	87.95(3)	88.12(3)	110.52(3)
$\gamma$ ( $^\circ$ )	67.67(3)	68.60(3)	90
$V$ (Å <sup>3</sup> )	1547.4(5)	1574.3(6)	2842.3(10)
$Z$	2	2	4
$T$ (K)	153	153	153
$\rho_{\text{calcd}}$ (g/cm <sup>3</sup> )	1.543	1.714	1.630
$\mu(\text{Mo K}\alpha)$ (cm <sup>-1</sup> )	17.34	38.84	30.86
$R_1(F)^a$	0.030	0.026	0.032
$R_w(F^2)^b$	0.103	0.072	0.077

$$^a R_1(F) = \frac{\sum |F_o| - |F_c|}{\sum |F_o|}$$

$$^b R_w(F^2) = \left[ \frac{\sum w(F_o^2 - F_c^2)^2}{\sum wF_o^4} \right]^{1/2}; w^{-1} = \sigma^2(F_o^2) + (qF_o^2)^2 \text{ for } F_o^2 > 0; w^{-1} = \sigma^2(F_o^2) \text{ for } F_o^2 \leq 0; q = 0.055 \text{ for } \mathbf{1}; q = 0.04 \text{ for } \mathbf{2} \text{ and } \mathbf{3}.$$

Table 2

Selected bond distances (Å) and angles (°) for  $\text{Cp}_2\text{Ce}[\eta^3\text{-N}(\text{SPPPh}_2)_2]$  (**1**),  $\text{Cp}_2\text{Ce}[\eta^3\text{-N}(\text{SePPh}_2)_2]$  (**2**), and  $\text{Cp}_2\text{Ce}[\eta^3\text{-N}(\text{SP}^i\text{Pr}_2)(\text{SePPh}_2)]$  (**3**)

	<b>1</b> <sup>a</sup>	<b>2</b> <sup>b</sup>	<b>3</b> <sup>c</sup>
Ce–Q(1)	2.988(1)	3.1083(8)	2.9747(9)
Ce–Q(2)	3.000(1)	3.1175(8)	3.0921(7)
Ce–N(1)	2.567(3)	2.594(2)	2.601(2)
Q(1)–P(1)	1.993(1)	2.149(1)	
Q(2)–P(2)	1.995(1)	2.1467(8)	
Q(1)–P(2)			1.998(1)
Q(2)–P(1)			2.149(1)
P(1)–N(1)	1.619(3)	1.622(2)	1.613(2)
P(2)–N(1)	1.617(3)	1.629(2)	1.631(2)
Q(1)–Ce–Q(2)	122.29(4)	125.56(3)	126.30(3)
N(1)–Ce–Q(1)	62.28(7)	63.46(5)	62.77(5)
N(1)–Ce–Q(2)	62.18(7)	63.47(5)	63.58(5)
P(1)–Q(1)–Ce	84.22(5)	80.92(3)	
P(2)–Q(2)–Ce	83.63(4)	80.48(3)	
P(1)–Q(2)–Ce			80.89(3)
P(2)–Q(1)–Ce			84.61(4)
P(1)–N(1)–Ce	107.4(1)	109.5(1)	108.8(1)
P(2)–N(1)–Ce	107.1(1)	108.88(9)	105.7(1)
P(1)–N(1)–P(2)	144.3(2)	141.1(1)	144.3(2)
N(1)–P(1)–Q(1)	106.1(1)	106.11(8)	
N(1)–P(2)–Q(2)	106.3(1)	106.33(7)	
N(1)–P(1)–Q(2)			106.32(9)
N(1)–P(2)–Q(1)			106.81(9)

<sup>a</sup> Q(1) = S(1), Q(2) = S(2).

<sup>b</sup> Q(1) = Se(1), Q(2) = Se(2).

<sup>c</sup> Q(1) = S(1), Q(2) = Se(1).

### 3. Results and discussion

#### 3.1. Syntheses

Reactions of equimolar amounts of  $\text{Cp}_3\text{Ce}$  and  $\text{HN}(\text{SPPPh}_2)_2$ ,  $\text{HN}(\text{SePPh}_2)_2$ , or  $\text{HN}(\text{SP}^i\text{Pr}_2)(\text{SePPh}_2)]$  in THF at 25 °C afforded  $\text{Cp}_2\text{Ce}[\eta^3\text{-N}(\text{SPPPh}_2)_2]$  (**1**),  $\text{Cp}_2\text{Ce}[\eta^3\text{-N}(\text{SePPh}_2)_2]$  (**2**), or  $\text{Cp}_2\text{Ce}[\eta^3\text{-N}(\text{SP}^i\text{Pr}_2)(\text{SePPh}_2)]$  (**3**), respectively. These compounds are soluble in THF and  $\text{CH}_2\text{Cl}_2$ . The yellow crystals of compounds **1–3** rapidly turn black when exposed to air. The compounds are water sensitive but they are stable under inert conditions and under paraffin oil for extended periods of time.

#### 3.2. NMR spectroscopy

NMR data for the present and related rare-earth compounds are given in Table 3. The  $^{31}\text{P}\{\text{H}\}$  NMR spectrum of **1** shows a singlet, shifted far downfield compared to the free ligand. The  $^{31}\text{P}\{\text{H}\}$  NMR spectrum of **2** shows a singlet with the expected  $^{77}\text{Se}$  satellites. The  $^{77}\text{Se}$  NMR spectrum of **2** shows a doublet that is shifted to a higher frequency compared to that in  $\text{HN}(\text{SePPh}_2)_2$ . A single  $^{31}\text{P}$  resonance is found in **1** and **2**. This indicates that in each compound the two P atoms are equivalent. The  $^{31}\text{P}\{\text{H}\}$  NMR spectrum of **3** shows two singlets: the peak at 18.7 ppm can be assigned to the P atom bonded to the S atom and the peak at –52.5 ppm can be assigned to the P atom bonded to the Se atom. The  $^{77}\text{Se}$  NMR spectrum of **3** shows a doublet with a typical  $^1J_{\text{Se-P}}$  coupling constant that is consistent with those in other metal-coordinated ligands. The characteristic shifts in the  $^{31}\text{P}$  NMR spectra to higher frequencies confirm complexation of these ligands. The  $^{31}\text{P}$  resonances in **1–3** are shifted to much lower frequencies compared to those in similar rare-earth compounds. Such behavior has been found previously in some rare-earth complexes containing the  $[\text{N}(\text{OPPh}_2)_2]^-$  ligand [14] and also in  $[\text{Ni}\{(\text{SPPPh}_2)_2\text{N-S,S'}\}_2] \cdot 2\text{THF}$  [15], where a  $^{31}\text{P}$  NMR chemical shift at –459 ppm is observed during the fast isomerization of square-planar to tetrahedral coordination. This  $^{31}\text{P}$  NMR trend in **1–3** is contrary to that found in most of the known transition-metal complexes containing these and related ligands. As is usual, the  $^{31}\text{P}$  resonances of the S-containing complexes are at higher frequencies compared to those containing Se.

#### 3.3. Structures

The molecular structures of  $\text{Cp}_2\text{Ce}[\eta^3\text{-N}(\text{SPPPh}_2)_2]$  (**1**),  $\text{Cp}_2\text{Ce}[\eta^3\text{-N}(\text{SePPh}_2)_2]$  (**2**), and  $\text{Cp}_2\text{Ce}[\eta^3\text{-N}(\text{SP}^i\text{Pr}_2)(\text{SePPh}_2)]$  (**3**) are shown in Figs. 1–3, respectively. In each structure, the ligand is coordinated to the  $\text{Cp}_2\text{Ce}$  moiety in an  $\eta^3$  fashion through the two chalcogen atoms and an N atom. This type of core geometry with  $\eta^3$  coordina-

Table 3

Selected NMR data for **1–3** and related rare-earth compounds

Compound	$^{31}\text{P}\{\text{H}\}$ (ppm)	$^1J_{\text{P-Se}}$ (Hz)	$^{77}\text{Se}\{\text{H}\}$ (ppm)	$^1J_{\text{Se-P}}$ (Hz)	$^2J_{\text{P-P}}$ (Hz)	Reference
$\text{HN}(\text{SPPPh}_2)_2$	56.9					ref. [8]
$\text{HN}(\text{SePPh}_2)_2$	52.3	790	–162.8	790	25	ref. [9]
$\text{HN}(\text{SP}^i\text{Pr}_2)(\text{SePPh}_2)$	99.1, 46.3	783	–224.9	782	28	ref. [11]
$\text{Cp}_2\text{Ce}[\eta^3\text{-N}(\text{SPPPh}_2)_2]$ ( <b>1</b> )	–40.6					this work
$\text{Cp}_2\text{Ce}[\eta^3\text{-N}(\text{SePPh}_2)_2]$ ( <b>2</b> )	–64.6	538	37.8	609		this work
$\text{Cp}_2\text{Ce}[\eta^3\text{-N}(\text{SP}^i\text{Pr}_2)(\text{SePPh}_2)]$ ( <b>3</b> )	–52.5, 18.7		86.6	590		this work
$\text{Cp}_2\text{Y}[\eta^3\text{-N}(\text{SPPPh}_2)_2]$	47.8					ref. [5]
$\text{Cp}_2\text{Y}[\eta^3\text{-N}(\text{SePPh}_2)_2]$	41.03	604	–126.8		66	ref. [5]
$\text{Y}[\eta^3\text{-N}(\text{SPPPh}_2)_2]_3$	42.5					ref. [7]
$\text{Y}[\eta^2\text{-N}(\text{SePPh}_2)_2]_2[\eta^3\text{-N}(\text{SePPh}_2)_2]$	32.4	581	33.9			ref. [7]
$\text{Cp}_2\text{Yb}[\eta^3\text{-N}(\text{SPPPh}_2)_2]$	74.1					ref. [6]
$\text{Cp}_2\text{Yb}[\eta^2\text{-N}(\text{SePPh}_2)_2]$	82.9	566				ref. [6]
$\text{Cp}_2\text{La}[\eta^3\text{-N}(\text{SePPh}_2)_2]$	37.1	610	–97.0	613		ref. [6]
$\text{Cp}_2\text{Er}[\eta^3\text{-N}(\text{SePPh}_2)_2]$	62.2					ref. [6]

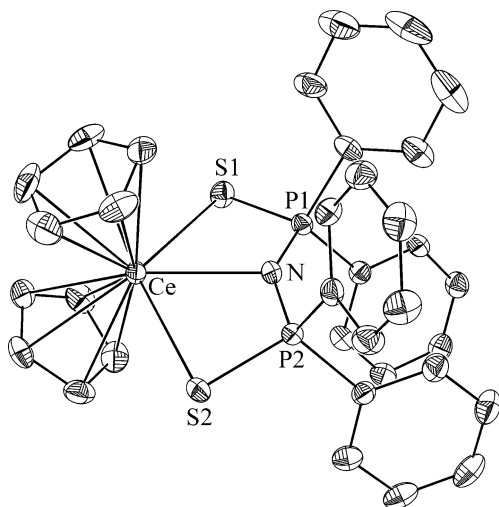


Fig. 1. Molecular structure of  $\text{Cp}_2\text{Ce}[\eta^3\text{-N}(\text{SPPH}_2)_2]$  (**1**). Here and in the succeeding figures anisotropic displacement parameters are drawn at the 50% probability level and H atoms have been omitted for the sake of clarity.

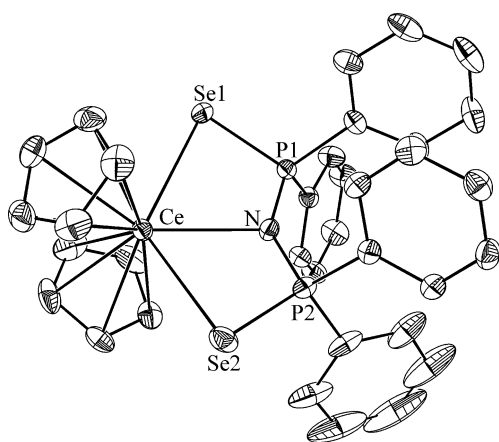


Fig. 2. Molecular structure of  $\text{Cp}_2\text{Ce}[\eta^3\text{-N}(\text{SePPh}_2)_2]$  (**2**).

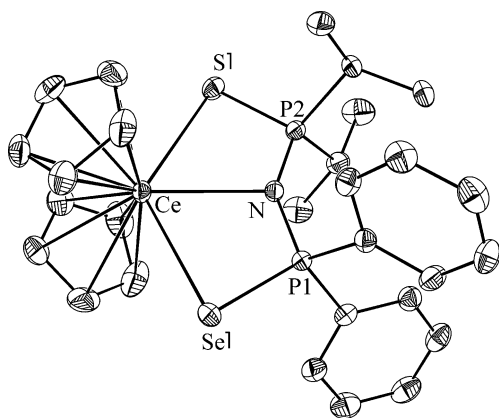


Fig. 3. Molecular structure of  $\text{Cp}_2\text{Ce}[\eta^3\text{-N}(\text{SP}'\text{Pr}_2)(\text{SePPh}_2)]$  (**3**).

tion is a common one among previously reported rare-earth compounds. Selected bond distances and angles are listed in Table 2.

Not surprisingly, the Ce–Se bond distances in **2** of 3.1083(8) and 3.1175(8) Å compare well with that of 3.0921(7) Å in **3**, where the same R groups are involved. Note that the Ce–S bond distances in **1** of 2.988(1) and 3.000(1) Å differ minimally from that of 2.9747(9) Å in **3**, despite the different R groups on S. These Ce–Se distances are in the range of the Ce–Se distances in  $\text{NaCeP}_2\text{Se}_6$  (3.0674(8)–3.4733(9) Å) [16] and in  $\text{Rb}_3\text{CeP}_2\text{Se}_8$  (3.014(1)–3.354(1) Å) [17]. As expected, the current Ce–Se distances are also consistent with Ln–Se distances in analogous compounds when the lanthanide contraction is taken into account. Thus, the Ln–Se distances are 3.108(1)–3.178(1) Å in  $[\text{THF}]_2\text{Sm}[\eta^3\text{-N}(\text{SePPh}_2)[\eta^2\text{-N}(\text{SePPh}_2)_2]$  [18], 3.052(2) and 3.053(2) Å in  $\text{Cp}_2\text{Y}[\eta^3\text{-N}(\text{SePPh}_2)_2]$  [5], 3.123(1) and 3.131(1) Å in  $\text{Cp}_2\text{La}[\eta^3\text{-N}(\text{SePPh}_2)_2]$ , 3.049(1) and 3.059(1) Å in  $\text{Cp}_2\text{Gd}[\eta^3\text{-N}(\text{SePPh}_2)_2]$ , and 3.020(1) and 3.037(1) Å in  $\text{Cp}_2\text{Er}[\eta^3\text{-N}(\text{SePPh}_2)_2]$  [6]. The Se–Ce–Se bond angle in **2** (125.56(3)°) is comparable to that in  $\text{NaCeP}_2\text{Se}_6$  (124.2(2)°) [16].

The Ce–S bond distances of 2.988(1) and 3.000(1) Å in **1** and that of 2.9747(9) Å in **3** are consistent with those of 2.921(1)–2.983(1) Å in  $[\text{Ce}(\kappa^2\text{-S}_2\text{CNMe}_2)_3(\text{THF})_2]$ , 2.906(1)–2.993(1) Å in  $[\text{Ce}(\kappa^2\text{-S}_2\text{CNMe}_2)_3(\text{bipy})_2]$  [19], 2.876(4)–2.936(4) Å in  $[\text{Ce}(\kappa^2\text{-S}_2\text{CNMe}_2)_3(\text{diphen})] \cdot 2\text{THF}$  [19], 2.949(1) and 2.983(1) Å in  $[\text{Ce}(\kappa^2\text{-S}_2\text{CNET}_2)_4]$  [19], and 3.004(8) and 3.005(8) Å in  $[\text{AsPh}_4][\text{Ce}(\text{S}_2\text{PMe}_2)_4]$  [20]. These Ce–S distances may be compared to the previously reported rare-earth metal complexes  $\text{Cp}_2\text{Y}[\eta^3\text{-N}(\text{SPPH}_2)_2]$  (2.928(2) and 2.935(2) Å) [5] and  $\text{Cp}_2\text{Yb}[\eta^3\text{-N}(\text{SPPH}_2)_2]$  2.882(1) and 2.940(1) Å [6]. The S–Ce–S bond angle in **1** (122.29(4)°) is comparable to that in  $[\text{AsPh}_4][\text{Ce}(\text{S}_2\text{PMe}_2)_4]$  (121.8(2)°).

The Ce–N bond distances in all three structures (2.567(3) Å for **1**, 2.594(2) Å for **2**, and 2.601(2) Å for **3**) are slightly shorter than the Ce–N distances in  $[\text{Ce}(\kappa^2\text{-S}_2\text{CNMe}_2)_3(\text{bipy})_2]$  (2.655(3) and 2.676(3) Å) and  $[\text{Ce}(\kappa^2\text{-S}_2\text{CNMe}_2)_3(\text{diphen})] \cdot 2\text{THF}$  (2.664(1) and 2.665(1) Å) [19].

The P–S, P–Se, and P–N bond distances in **1–3** are typical of those reported for metal-coordinated ligands.

## Acknowledgment

This work was supported in part by the US National Science Foundation (Grant No. CHE-9819385).

## Appendix A. Supplementary data

CIF format crystallographic files for  $\text{Cp}_2\text{Ce}[\eta^3\text{-N}(\text{SPPH}_2)_2]$  (**1**),  $\text{Cp}_2\text{Ce}[\eta^3\text{-N}(\text{SePPh}_2)_2]$  (**2**) and  $\text{Cp}_2\text{Ce}[\eta^3\text{-N}(\text{SP}'\text{Pr}_2)(\text{SePPh}_2)]$  (**3**) have been deposited with the Cambridge Crystallographic Data Centre, CCDC Nos. 285216, 285217, and 285218, respectively. Copies may be obtained free of charge from The Director, CCDC, 12 Union Road, Cambridge, CB2 1EZ, UK, fax: +44 1223 336 033; e-mail: deposit@ccdc.cam.ac.uk or <http://www.ccdc.cam.ac.uk>. Supplementary data associated with

this article can be found, in the online version, at [doi:10.1016/j.ica.2005.10.029](https://doi.org/10.1016/j.ica.2005.10.029).

## References

- [1] M. Bochmann, *Chem. Vapor. Depos.* 2 (1996) 85.
- [2] D.J. Crouch, P. O'Brien, M.A. Malik, P.J. Skabara, S.P. Wright, *Chem. Commun.* (2003) 1454–1455.
- [3] D.J. Crouch, M. Helliwell, P. O'Brien, J.-H. Park, J. Waters, D.J. Williams, *J. Chem. Soc., Dalton Trans.* (2003) 1500.
- [4] M. Afzaal, D. Crouch, M.A. Malik, M. Motevalli, P. O'Brien, J.-H. Park, *J. Mater. Chem.* 13 (2003) 639.
- [5] C.G. Pernin, J.A. Ibers, *Inorg. Chem.* 38 (1999) 5478.
- [6] C.G. Pernin, J.A. Ibers, *Inorg. Chem.* 39 (2000) 1216.
- [7] C.G. Pernin, J.A. Ibers, *Inorg. Chem.* 39 (2000) 1222.
- [8] F.T. Wang, J. Najdzionek, K.L. Leneker, H. Wasserman, D.M. Braitsch, *Synth. React. Inorg. Met. Org. Chem.* 8 (1978) 119.
- [9] P. Bhattacharyya, J. Novosad, J. Phillips, A.M.Z. Slawin, D.J. Williams, J.D. Woollins, *J. Chem. Soc., Dalton Trans.* (1995) 1607.
- [10] P. Bhattacharyya, A.M.Z. Slawin, D.J. Williams, J.D. Woollins, *J. Chem. Soc., Dalton Trans.* (1995) 2489.
- [11] P. Sekar, J.A. Ibers, *Inorg. Chem.* 42 (2003) 6294.
- [12] Bruker SMART Version 5.054 Data Collection and SAINT-Plus Version 6.45a Data Processing Software for the SMART System. (Bruker Analytical X-Ray Instruments, Inc., Madison, WI, USA, 2005).
- [13] G.M. Sheldrick, *SHELXTL Version 6.14*, Bruker Analytical X-Ray Instruments, Inc., Madison, WI, USA, 2003.
- [14] P. Rubini, C.B. Nasr, L. Rodehüser, J.-J. Delpuech, *Magn. Reson. Chem.* 25 (1987) 609.
- [15] E. Simón-Manso, M. Valderrama, D. Boys, *Inorg. Chem.* 40 (2001) 3647.
- [16] J.A. Aitken, M. Evain, L. Iordanidis, M.G. Kanatzidis, *Inorg. Chem.* 41 (2002) 180.
- [17] K. Chondroudis, M.G. Kanatzidis, *Inorg. Chem.* 37 (1998) 3792.
- [18] M. Geissinger, J. Magull, *Z. Anorg. Allg. Chem.* 623 (1997) 755.
- [19] P.B. Hitchcock, A.G. Hulkes, M.F. Lappert, Z. Li, *J. Chem. Soc., Dalton Trans.* (2004) 129.
- [20] S. Spiliadis, A.A. Pinkerton, D. Schwarzenbach, *J. Chem. Soc., Dalton Trans.* (1982) 1809.